Liquid Crystals

Publication details, including instructions for authors and subscription information:
http://www.informaworld.com/smpp/title~content=t713926090

Liquid crystal alignment properties of *n*-alkylsulphonylmethyl-substituted polyoxyethylenes

Hyo Kang[a]; Eun-Ho Sohn[a]; Daeseung Kang[b]; Jong-Chan Lee[a]
[a] Department of Chemical and Biological Engineering, Seoul National University, Gwanak-gu, Seoul, Korea [b] Department of Electrical Engineering, Soongsil University, Dongjak-Gu, Seoul, Korea

To cite this Article Kang, Hyo , Sohn, Eun-Ho , Kang, Daeseung and Lee, Jong-Chan(2009) 'Liquid crystal alignment properties of *n*-alkylsulphonylmethyl-substituted polyoxyethylenes', Liquid Crystals, 36: 8, 855 — 864

To link to this Article: DOI: 10.1080/02678290903078859

URL: http://dx.doi.org/10.1080/02678290903078859

Liquid Crystals,
Vol. 36, No. 8, August 2009, 855–864

Taylor & Francis
Taylor & Francis Group

Liquid crystal alignment properties of *n*-alkylsulphonylmethyl-substituted polyoxyethylenes

Hyo Kang[a], Eun-Ho Sohn[a], Daeseung Kang[b] and Jong-Chan Lee[a]*

[a]*Department of Chemical and Biological Engineering, Seoul National University, 599 Gwanangno, Gwanak-gu, Seoul 151-742, Korea;* [b]*Department of Electrical Engineering, Soongsil University, 511 Sangdo-Dong, Dongjak-Gu, Seoul 156-743, Korea*

(Received 21 May 2009; accepted 29 May 2009)

The liquid crystal (LC) alignment properties of LC cells fabricated with films of *n*-alkylsulphonylmethyl-substituted polyoxyethylenes (#S-PEO, # = 4, 6, 7, 8 and 10), where # is the number of carbon atoms in the *n*-alkyl side groups having different *n*-alkyl chain length, were investigated as a function of the rubbing density. The LC cells made from unrubbed #S-PEO (# $\geq$8) films having more than eight carbon atoms in the *n*-alkyl side groups showed homeotropic LC alignment. The homeotropic LC alignment behaviour correlated well with the surface energy values of the unrubbed #S-PEO films; homeotropic LC alignment was observed when the surface energy values of the unrubbed #S-PEO films were smaller than about 21.62 mJ m^{-2}. The LC cells made from rubbed #S-PEO (# $\geq$7) films having more than seven carbon atoms with a rubbing density of 150 showed homeotropic LC alignment. It was also found that the tilt angle of the LCs on the rubbed #S-PEO films was affected not only by the *n*-alkyl chain length of the polymers, but also by the rubbing density, regardless of the surface energy value of the #S-PEO film.

Keywords: liquid crystal; alignment; polyoxyethylene; rubbing

1. Introduction

The uniform alignment of liquid crystal (LC) molecules on polymeric alignment layers is very important for the fabrication of high quality LC displays (*1–11*). The mechanical rubbing of polymeric substrates is the most widely used technique to produce uniform LC alignment, due to its simplicity and rapidity (*1–3*). The LC alignment properties are highly affected by the chemical structures of the substrate materials (*1*, *2*, *12–15*). In particular, the length of the alkyl groups in the substrate materials was found to produce different LC alignment behaviour in studies of LC cells made from polyimides (*16–22*), polystyrenes (*23*, *24*), polythiophenes (*25*) and self-assembled monolayers (*26*) as the alignment layers.

Recently, we synthesised a series of *n*-alkylsulphonylmethyl-substituted polyoxyethylenes (#S-PEO) with different alkyl groups shown in Figure 1. These polymers were found to be well ordered on their surface according to the characterisation of their thin films using X-ray reflectivity and near-edge X-ray absorption fine structure (NEXAFS) spectroscopy (*27–32*). In this study, we systematically investigated the alignment properties of the LC cells made from rubbed #S-PEO films with different *n*-alkyl groups having 4 to 10 carbons. The surface properties of the #S-PEO films and optical properties of the LC cells were also investigated.

2. Experimental

2.1 Material

n-Alkylsulphonylmethyl-substituted polyoxyethylenes (#S-PEO, # = 4, 6, 7, 8 and 10), where # and S represent the number of carbons in the *n*-alkyl side group and the sulphonyl group, respectively, were prepared as previously reported (*27*–29). Properties of the #S-PEOs are listed in Table 1. 4-*n*-Pentyl-4′-cyanobiphenyl (5CB, n_e = 1.736, n_o = 1.5442, and $\Delta\varepsilon$ = 14.5, where n_e, n_o and $\Delta\varepsilon$ represent extraordinary refractive indexes, ordinary refractive indexes and dielectric anisotropy, respectively) was purchased from Merck Co. *N,N′*-Dimethylacetamide and ethanol were dried over molecular sieves (4 Å). All other reagents and solvents were used as received from Aldrich.

2.2 Film preparation and LC alignment process

Solutions of the polymers in tetrahydrofuran (THF) (0.5 wt%) were filtered using a polytetrafluoroethylene membrane with a pore size of 0.45 μm. Thin films of the polymers were prepared by spin-coating (2000 rpm, 30 seconds) on to 1.5 cm × 1.5 cm indium tin oxide (ITO)-coated glass and 1.5 cm × 2.0 cm polyethylene terephthalate (PET) substrates. The polymer films were rubbed using a rubbing machine (RMS-50-M, Nam Il Optical Components Corp., Incheon, Korea). The

---

*Corresponding author. Email: jongchan@snu.ac.kr

ISSN 0267-8292 print/ISSN 1366-5855 online

DOI: 10.1080/02678290903078859
http://www.informaworld.com

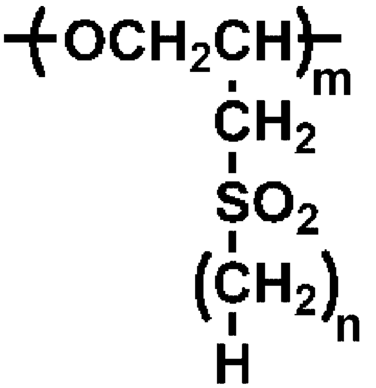

$\mathrm{-\!\!(OCH_2CH(CH_2SO_2(CH_2)_nH))_m\!\!-}$

#S-PEO

n= 4, 6, 7, 8, and 10

Figure 1. Chemical structures of the polymers (#S-PEO), where # indicates the number of carbon atoms in the *n*-alkyl side groups of the polymers.

Table 1. Characterisation results for the synthesis of the #S-PEO films.

Polymer designation	M_n[a]	M_w/M_n[a]	T_g (°C)[b]	Endotherms[b] (°C)	ΔH (J g^{-1})[b]
4S-PEO	16,600	1.60	32		
6S-PEO	20,700	1.68	56	100	15.7
7S-PEO	47,000	2.81	56	135	17.6
8S-PEO	51,900	2.42	63	150	17.6
				116	4.6
10S-PEO	33,200	4.04	65	164	13.8

[a] Obtained from gel permeation chromatography using tetrahydrofuran as solvent with respect to monodisperse polystyrene as standard.

[b] Measured from second heating using differential scanning calorimeter.

rubbing density equation is written as $L/l = N[(2\pi rn/60v)-1]$, where L is the total length of the rubbing cloth (mm), l is the contact length of the circumference of the rubbing roller (mm), N is the cumulative number of rubbings, n is the speed (rpm) of the rubbing roller, r is the radius (cm) of the rubbing roller, and v is the velocity (cm s^{-1}) of the substrate stage (*33*, *34*).

2.3 *LC cell assembly*

Antiparallel LC cells were fabricated using the unrubbed or rubbed polymer films on to ITO-coated glass and PET substrates. The antiparallel LC cells were constructed by assembling the unrubbed or rubbed polymer films together antiparallel with respect to the rubbing direction using spacers with thicknesses of 4.25 μm and 50 μm. The fabricated LC cells were filled with a nematic LC, 5CB, in isotropic state in order to avoid creating flow alignment by capillary action. The manufactured LC cells were sealed with epoxy.

2.4 *Instrumentation*

^{1}H nuclear magnetic resonance measurements were carried out on a JEOL JNM-LA at 300 MHz. Gel permeation chromatography (GPC) was used to measure the number average molecular weight (M_n) and molecular weight distributions (M_w/M_n) of synthesised polymer with respect to polystyrene standards using THF as an eluent and a UV detector. Differential scanning calorimeter (DSC) measurements were carried out on TA instruments 2920 at a heating and cooling rate of 10°C min^{-1} under a nitrogen atmosphere. The topography of the unrubbed, rubbed polymer films in an area of 3 μm × 3 μm was examined using atomic force microscopy (AFM) (SPA-400, Seiko Instruments Inc.) in tapping mode (spring constant of the cantilever: 0.6 N m^{-1}, scan rate: 1 Hz). Surface roughness (R_a) values of the polymer films using AFM were less than 3 nm. The contact angles of distilled water and methylene iodide on polymer films were determined with a Kruss DSA10 contact angle analyser equipped with drop shape analysis software. The surface energy value was calculated using the Owens-Wendt's equation as

$$\gamma_{sl} = \gamma_s + \gamma_l - 2(\gamma_s^d\gamma_l^d)^{1/2} - 2(\gamma_s^p\gamma_l^p)^{1/2}$$

where γ_l is the surface energy of the liquid, γ_{sl} is the interfacial energy of the solid/liquid interface, γ_s is the surface energy of the solid, γ_l^d and γ_l^p are known for the test liquids, γ_s^d and γ_s^p can be calculated from the measured static contact angles (*35*). Two-dimensional grazing incidence X-ray diffraction (GIWAXD) measurements were carried out on the 4C2 beam line at the Pohang Accelerator Laboratory in Korea (wavelength: 1.3807 Å). The diffraction pattern was recorded using a two-dimensional image detector (PI-SCX4300-165/2, Princeton Instruments, Trenton, NJ, USA). The incidence angles were about 0.17–0.20°. Electron spectroscopy for chemical analysis (ESCA) was carried out using a constant analyser energy mode employing Al K_α source (100.0 eV). The spectra were obtained at a take-off angle of 90°. The LC alignment direction of the antiparallel LC cells was investigated by measuring the angular dependence of absorbance of dichroic dye (disperse blue 1, Aldrich), which was dissolved in 5CB at a concentration of 1 wt%, using optical apparatus equipped with a He-Ne laser, a polariser and a photodiode detector as a function of rotation angle of samples (*34*). The tilt angle of LCs with respect to the planar direction of antiparallel LC cells was measured by the crystal rotation method (*36*). The cell gap was measured before filling the LCs using a spectrophotometer (S2000, Ocean Optics Inc., Dunedin, FL, USA). The polarised optical microscopy (POM) images of LC cells were observed from an optical microscope (ECLIPSE E600 POL, Nikon) equipped with a polariser and digital camera (COOLPIX995, Nikon).

3. Results and discussion

Figure 1 shows the chemical structures of the *n*-alkylsulphonylmethyl-substituted polyoxyethylenes (#S-PEO, # = 4, 6, 7, 8 and 10). The number average molecular weights (M_n) of 4S-PEO, 6S-PEO, 7S-PEO, 8S-PEO and 10S-PEO obtained by GPC were 16,600, 20,700, 47,000, 51,900 and 33,200, respectively. The thermal properties of these polymers were investigated by DSC (Table 1 and Figure 2). The polymer 4S-PEO was found to be amorphous, since only the glass transition temperature (T_g) was observed in its DSC curve, while 6S-PEO, 7S-PEO, 8S-PEO and 10S-PEO were found to be have side chain crystalline phases with melting transition (T_m) peaks. As the number of carbon atoms increased from 4 (4S-PEO) to 10 (10S-PEO), the T_g of #S-PEO increased from 32°C to 65°C. The increase of T_g was ascribed to the increased van der Waals interactions between the long alkyl groups, which cause them to act as a filler. As the number of carbon atoms increased from 6 to 10, the T_m and enthalpy of melting (ΔH) of #S-PEO increased from 100°C to 164°C and from 15.7 J g^{-1} to 18.4 J g^{-1}, respectively, which is a general phenomenon for comb-like polymers, because of the increase in the ordering of the side chains (*37*, *38*). Conclusively, as the number of carbon atoms in the *n*-alkyl side groups increases, the T_g, T_m and ΔH values of the polymers increase. More detailed information about their synthesis and characterisation was reported previously (*28*, *29*, *32*).

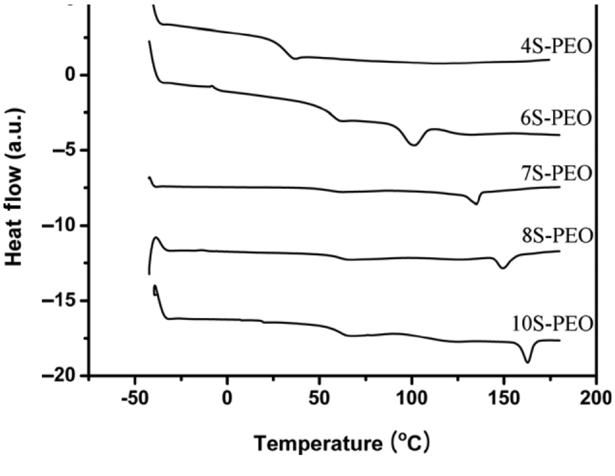

Figure 2. Differential scanning calorimeter thermograms of the polymers.

The LC aligning ability was observed from antiparallel LC cells by observing the POM images and transmitted intensity of a linearly polarised He-Ne laser beam passed through the LC cells as a function of the rotation angle of the samples. Figure 3 shows the orthoscopic and conoscopic (inlet) POM images of the LC cells made from the unrubbed or rubbed films of the #S-PEOs. When the rubbing density is 0 (unrubbed LC cells), 4S-PEO and 6S-PEO show random planar LC alignment, 7S-PEO shows random tilted LC alignment, and 8S-PEO and 10S-PEO show homeotropic LC alignment, indicating that the homeotropic LC aligning ability increases with increasing number of carbon atoms in the *n*-alkyl side groups. The LC cells fabricated with the 4S-PEO films always show poor LC alignment behaviour, even when the polymer films are rubbed with a high rubbing density of 250. When the rubbing density of the LC cell made from 6S-PEO was increased from 0 to 250, the random planar LC alignment observed at a rubbing density of 0 was changed to planar and parallel LC alignment with respect to the rubbing direction having low anchoring stability, slightly tilted alignment and finally, planar alignment at rubbing densities of 50, 150 and 250, respectively. Interestingly, the LC cell made from 7S-PEO at a rubbing density of 150 exhibits uniformly oriented homeotropic LC alignment, as shown in the conoscopic POM images in Figure 3, which changed to tilted alignment when the rubbing density was further increased to 250. All of the LC cells made from the 8S-PEO and 10S-PEO films with rubbing densities ranging from 0 to 250 invariably produced stable homeotropic LC alignment and the alignment property was maintained for at least 6 months, since the LC cells were first made from these polymers, as shown by the polar diagrams in Figure 4.

The tilt angles of the antiparallel LC cells fabricated with the #S-PEO films using 5CB were measured to study the effect of the rubbing density on LC alignment direction (Figure 5). The tilt angles of the 4S-PEO films could not be measured, due to the poor LC alignment on both the unrubbed and rubbed films. The tilt angles on the rubbed 6S-PEO films with a rubbing density of less than 50 could not be measured either, due to their poor LC alignment, and that on the rubbed 6S-PEO film with a rubbing density of 50 was about 0°. As the rubbing density increases from 50 to 250, the tilt angle of the LCs on the rubbed 6S-PEO film increases from 0° to 18°, then

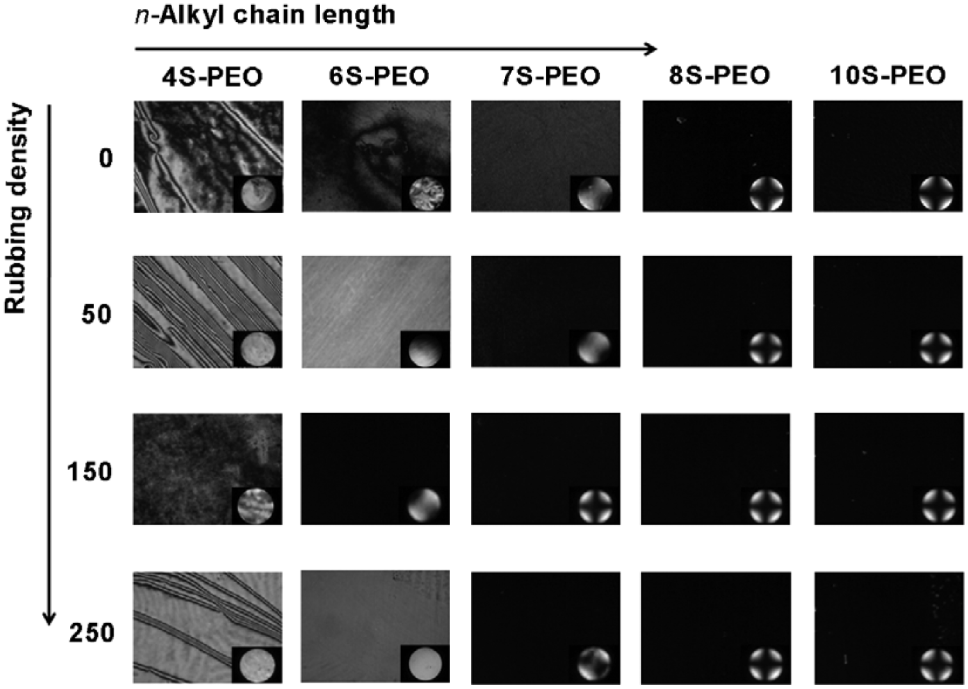

Figure 3. Orthoscopic and conoscopic (inlet) polarised optical microscopy images for the LC cells made from #S-PEO films according to the rubbing density.

decreases to 0°. Similarly, the tilt angles of the LCs on the rubbed 7S-PEO films with rubbing densities of 50, 150 and 250 were 75°, 90° and 30°, respectively. Therefore, the maximum tilt angles of the LC cells made from the rubbed 6S-PEO and 7S-PEO films were obtained at a rubbing density of 150. The tilt angles of the LC cells made from the unrubbed 8S-PEO and 10S-PEO films were found to be about 90°. Those of the LC cells made from the rubbed 8S-PEO and 10S-PEO films with a rubbing density of 250 were about 89°, indicating that the #S-PEO films with longer *n*-alkyl groups maintain their homeotropic LC alignment properties even at a very high rubbing density.

We tried to explain the changes in tilt angles of the LCs on the 6S-PEO and 7S-PEO films according to the rubbing density using several surface characterisation techniques, namely contact angle measurements, ESCA, GIWAXD and NEXAFS spectroscopy. We found that the contact angle and ESCA results were not affected by rubbing density, as shown in Tables 2 and 3. The AFM images of the rubbed #S-PEO films with different rubbing densities were also found to be very similar. Seo *et al.* (*39*) recently investigated the changes in the tilt angle of LCs on ion beam-treated polyimide with a long alkyl side chain using NEXAFS spectroscopy. We also believed that the somewhat different orientation of alkyl chain including the tilt angles of alkyl chain with respect to the surface normal could affect the tilt angles of LCs on the 6S-PEO and 7S-PEO films according to the rubbing density. Therefore, we also tried to measure the NEXAFS spectra of the rubbed 6S-PEO and 7S-PEO films with different rubbing densities to determine whether the surface orientation changes of the *n*-alkyl groups were responsible for the differences in the tilt angles. Unfortunately, we could not obtain any reproducible NEXAFS results from the rubbed films of 6S-PEO and 7S-PEO, possibly due to the mechanical scratched surface of the films in the rubbing process. Similarly GIWAXD results were also not reproducible. On the other hand, the ion beam-treated polyimide should not have such surface problems. Therefore, we failed to clarify the reason for the changes of tilt angles on rubbed 6S-PEO and 7S-PEO films, while the increase in tilt angles or improvement in the homeotropic alignment stability with increasing number of carbon atoms in the *n*-alkyl side group of the #S-PEOs was able to be explained by surface characterisation techniques, as follows.

Table 2 shows the surface energy values of the polymer films obtained based on the static contact angles of distilled water and methylene iodide. The total surface energy values of 4S-PEO, 6S-PEO, 7S-PEO, 8S-PEO and 10S-PEO are 32.43, 23.40, 22.34, 21.62 and 21.13 mJ m^{-2}, respectively, indicating that the surface energy decreases with increasing number of carbon atoms in the *n*-alkyl side groups (Figure 6). The surface energy values of

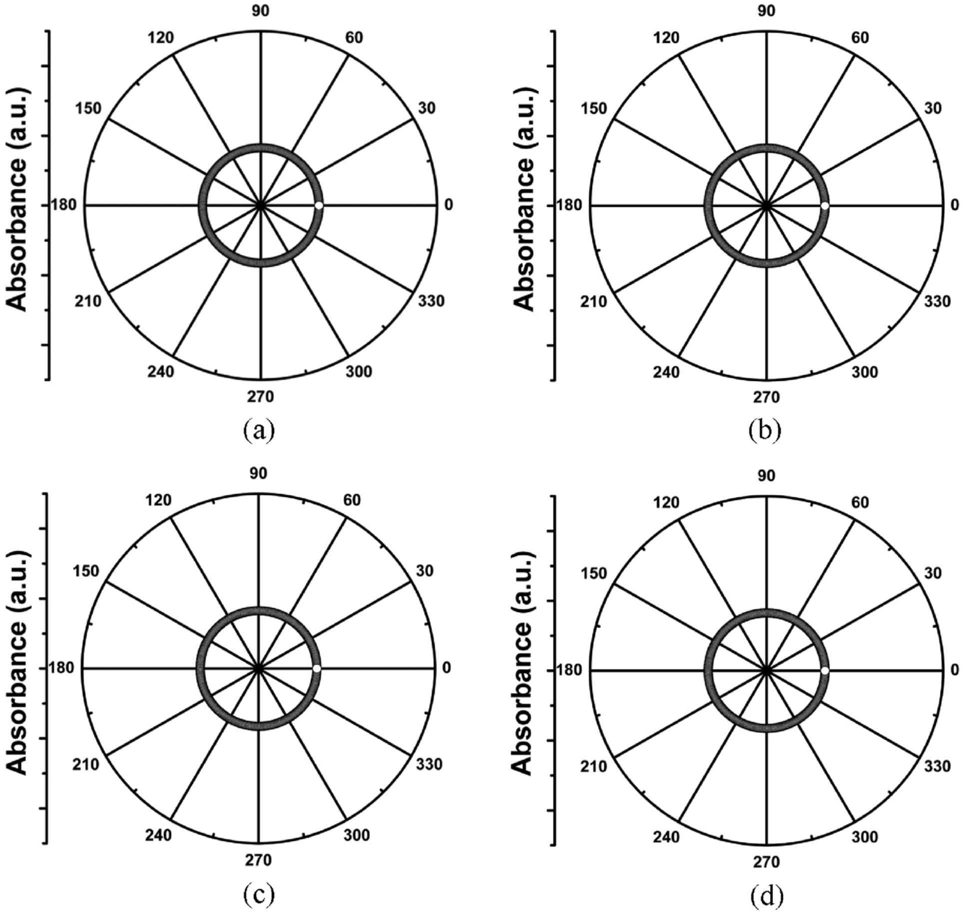

(a)

(b)

(c)

(d)

Figure 4. Polar diagrams of the absorbance of a disperse blue 1 in antiparallel LC cells fabricated with polymer films as a function of rotation angle of the samples. (a) 8S-PEO and (b) 10S-PEO are obtained just after the LC cells are prepared and (c) 8S-PEO and (d) 10S-PEO are obtained after 6 months.

the 8S-PEO and 10S-PEO films, which produce very stable homeotropic LC alignment, are comparable to those of fluorinated polymers such as poly(tetrafluoroethylene) and silicon resins such as poly(dimethylsiloxane) that are known to have the lowest surface energy values among all of the commercial synthetic polymers (*40*). The very low surface energy of #S-PEO was ascribed to the well oriented *n*-alkylsulphonylmethyl side groups producing effective packing structures of CH_3 groups on the top of the polymer surface (*31*). We performed ESCA studies of the #S-PEO films in order to measure the chemical composition of the polymer surfaces (Figure 6(a)–(c)). As expected, a decrease in the ratio of sulphur to carbon (S/C ratio) was observed with increasing number of carbon atoms in the *n*-alkyl side groups. Therefore, the #S-PEO films with longer *n*-alkyl side groups, which produced very stable homeotropic LC alignment, have higher carbon contents on their surface and lower surface energy values. The S/C ratio values obtained from the experiments were found to be always larger than the calculated ones, because the polar sulphone groups are included in the well-oriented *n*-alkylsulphonylmethyl side groups, which can increase the S content on the surface.

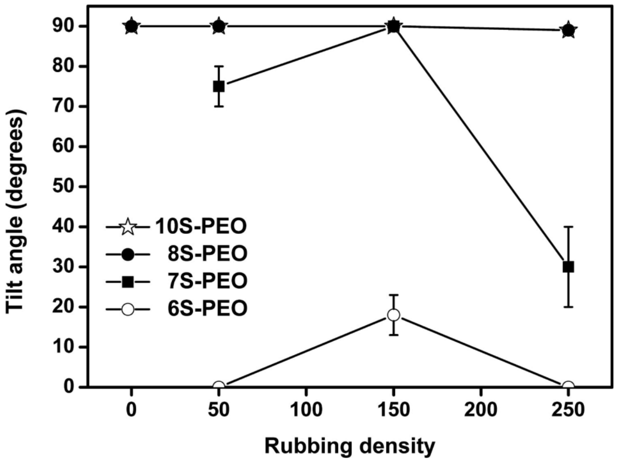

Figure 5. Tilt angles of the antiparallel LC cells fabricated with rubbed #S-PEO films as a function of rubbing density.

Table 2. Surface energy value, homeotropic liquid crystal aligning ability, *d*-spacing and sulphur/carbon ratio of unrubbed #S-PEO films.

Polymer designation	Surface energy (mJ m^{-2})[a]	Homeotropic LC aligning ability[b]	*d*-Spacing[c]	S/C (theoretical)	S/C[d] (experimental)
4S-PEO	32.43	X		0.143	0.160
6S-PEO	23.40	X	21.58	0.111	0.124
7S-PEO	22.34	X	23.87	0.100	0.113
8S-PEO	21.62	O	26.25	0.091	0.100
10S-PEO	21.13	O	30.28	0.077	0.083

[a] Calculated from Owens-Wendt's equation using the static contact angle of distilled water and methylene iodide.

[b] Circle (O) and cross (X) indicate that unrubbed polymer films have a homeotropic and poor LC aligning ability, respectively.

[c] *d*-Spacings of the first order reflection of polymers using grazing incidence X-ray diffraction.

[d] The S/C in #S-PEO at the take-off angle of 90° calculated from these S_{1s} and C_{1s} peaks in the electron spectroscopy for chemical analysis spectra.

Table 3. Surface energy value and sulphur/carbon ratio of rubbed #S-PEO film according to the rubbing density.

		Contact angle (o)[a]		Surface energy (mJ m^{-2})[b]			
Polymer designation	Rubbing density	Water	Methylene iodide	Dispersion	Polar	Total	S/C[c]
4S-PEO	50	76.5	65.8	20.59	11.63	32.22	
	150	76.7	66.0	20.50	11.56	32.06	
	250	76.6	65.7	20.66	11.54	32.20	
6S-PEO	50	94.2	73.6	18.49	4.15	22.63	0.123
	150	94.5	73.7	18.47	4.05	22.52	0.123
	250	94.3	73.7	18.44	4.12	22.57	0.120
7S-PEO	50	96.6	73.2	19.04	3.22	22.25	0.118
	150	97.0	73.6	18.86	3.14	21.99	0.119
	250	96.5	73.1	19.08	3.24	22.32	0.120
8S-PEO	50	98.0	74.0	18.76	2.86	21.62	0.100
	150	98.2	74.1	18.73	2.81	21.54	0.103
	250	98.2	74.3	18.61	2.84	21.45	0.100
10S-PEO	50	100.4	74.0	18.96	2.17	21.13	
	150	100.7	74.5	18.82	2.13	20.95	
	250	100.7	74.5	18.82	2.13	20.95	

[a] Measured from static contact angles.

[b] Calculated from Owens-Wendt's equation.

[c] The S/C in #S-PEO at the take-off angle of 90° calculated from these S_{1s} and C_{1s} peaks in the electron spectroscopy for chemical analysis spectra.

The two-dimensional GIWAXD study of the unrubbed #S-PEO films was carried out in order to investigate the effect of surface ordering on the LC alignment properties on the polymer surfaces (Figure 7). The 4S-PEO film does not show scattering spots indicating that its surface is not ordered at all. On the other hand, well-ordered scattering signals were observed along the out of plane direction, corresponding to the (001), (002) and (003) indices of the periodic lamellar layer spacings from the 6S-PEO, 7S-PEO, 8S-PEO and 10S-PEO films. These scattering spots indicate the presence of a layered structure stacked normal to the #S-PEO (# $\geq$6) film plane. The *d*-spacings of the first order reflection of 6S-PEO, 7S-PEO, 8S-PEO and 10S-PEO, calculated from a clear signal in the small angle regime, namely 21.58, 23.87, 26.25 and 30.28 Å, respectively, are approximately twice the expected length of the side chains calculated based on assumption that they are fully extended with the trans conformations (Table 2). Therefore, the 4S-PEO film having a poorly ordered surface structure did not produce any stable LC alignment layers at all. The 6S-PEO and 7S-PEO films having relatively low surface energy values and quite well-ordered surface structures are able to produce LC alignment layers when they are properly rubbed. The well-ordered surfaces of 8S-PEO and 10S-PEO having very low surface energy values are able to produce very stable homeotropic LC layers, regardless of the rubbing density.

Figure 8 shows the POM images of the LC cells fabricated with the 10S-PEO films heated for 10 minutes at various temperatures (60, 70, 80, 90, 100, 110 and 120°C). 10S-PEO was chosen as the LC alignment layer for the thermal stability test because this polymer

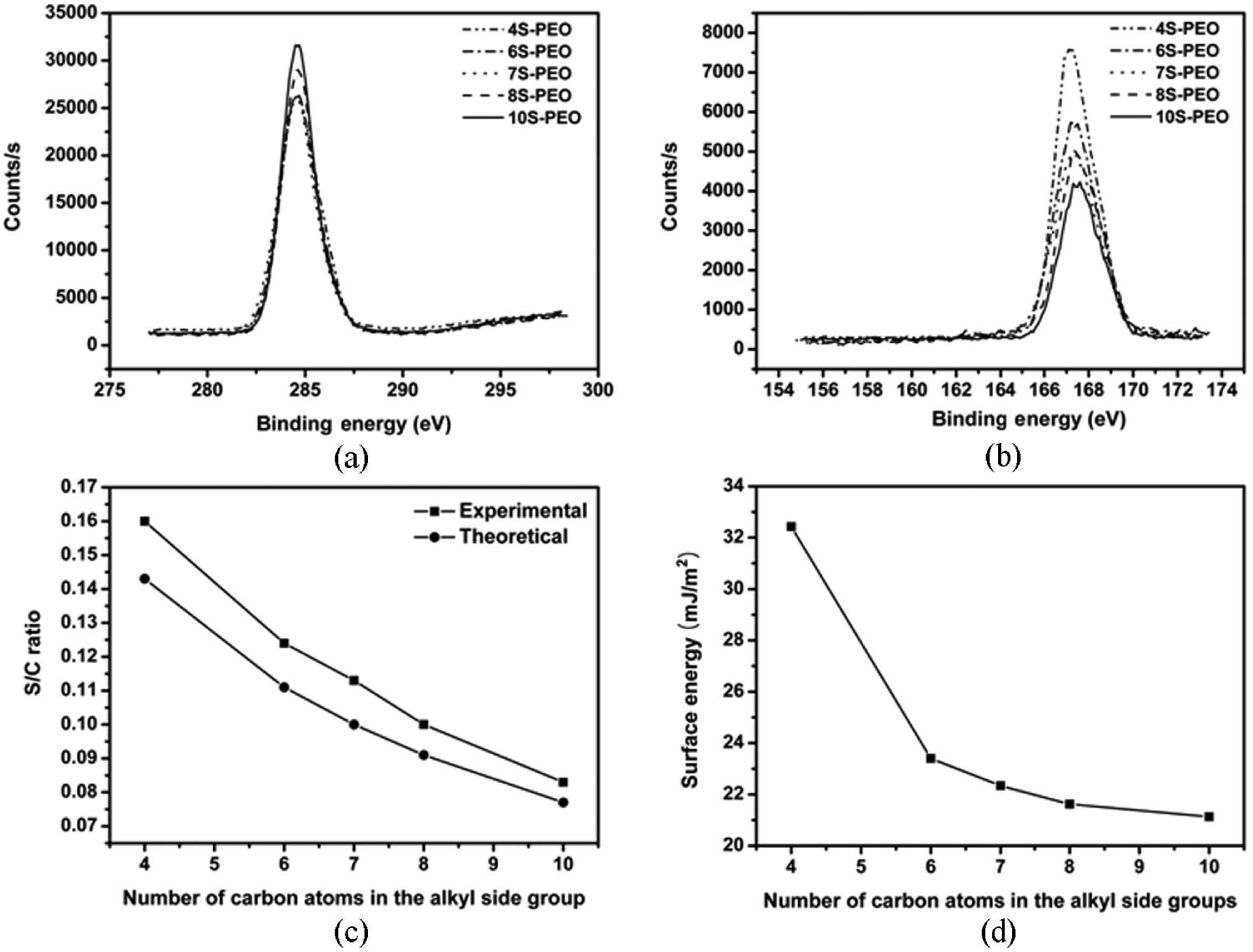

(a) (b)

(c) (d)

Figure 6. Electron spectroscopy for chemical analysis spectra of #S-PEO in (a) C_{1s}, (b) S_{1s} recorded at 90° take-off angle, (c) experimental, theoretical S_{1s}/C_{1s} ratio, and (d) surface energy value of #S-PEO films according to the number of carbon atoms in the alkyl side groups.

has longer alkyl side groups, which is also favourable for homeotropic LC alignment. Moreover, 10S-PEO has the highest T_g value among all of the polymers in this study, so that the polymer surface in the LC cell would be expected to exhibit better thermal stability. The homeotropic LC alignment behaviour of the LC cell was found to be maintained when it was heated for 10 minutes at 70°C (Figure 8(b)). Although its T_g is about 65°C, the molecular motion on the surface of 10S-PEO heated at 70°C for 10 minutes is insufficient to disturb the orientation of the LC molecules However, defects of the LC alignment were observed in the LC cells heated at 80, 90, 100 and 110°C, as shown in Figure 8(c)–(f), respectively, and totally random LC orientation was observed in the LC cell heated at 120°C for 10 minutes (Figure 8(g)). Therefore, the processing temperature of 10S-PEO for LC display applications should be below 70°C.

Recently, considerable effort has been made to develop plastic substrates for flexible LC displays (*41*). It was reported that #S-PEOs have good interfacial adhesion properties between the polymers and glass/plastic substrates (*42*). All of the LC cells made from the unrubbed #S-PEO films on PET substrates exhibit similar LC alignment behaviour to those made from the same polymer films on glass substrates. We found that the LC cells fabricated using the unrubbed 8S-PEO and 10S-PEO films on plastic (PET) substrates showed good homeotropic LC alignment behaviour. For example, the photo images of the unbent and bent LC cell made from the 10S-PEO film on the PET substrate clearly show homeotropic LC alignment behaviour (Figure 9). Furthermore, this LC cell showed very nice homeotropic LC aligning ability with a high tilt angle of about 90°,which was maintained after bending 100 times. Therefore, #S-PEOs can be considered as candidate LC alignment layers for flexible LC displays, such as in vertical alignment mode applications.

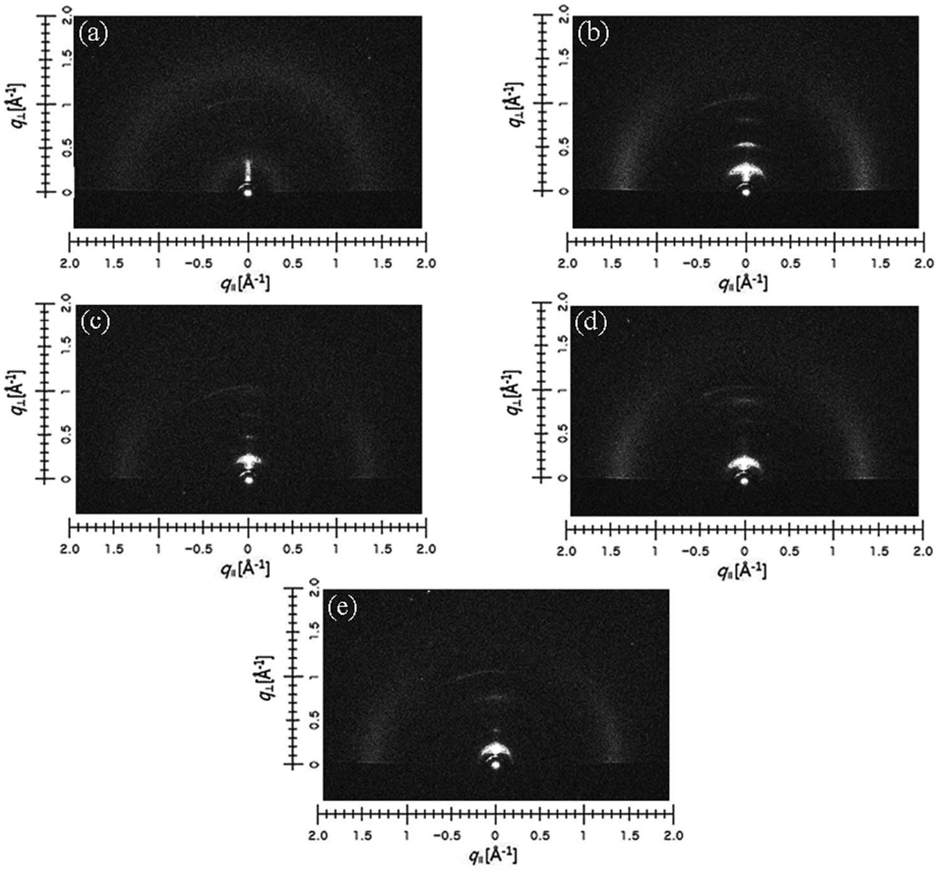

Figure 7. Grazing incidence X-ray diffraction patterns of the #S-PEO films: (a) 4S-PEO, (b) 6S-PEO, (c) 7S-PEO, (d) 8S-PEO and (e) 10S-PEO).

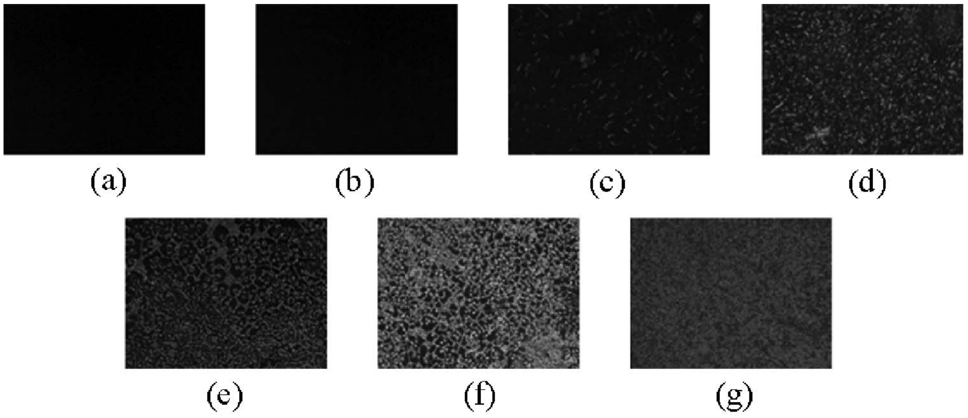

Figure 8. Polarised optical microscopy images of the LC cells made from unrubbed #S-PEO films annealed for 10 minutes at: (a) 60°C, (b) 70°C, (c) 80°C, (d) 90°C, (e) 100°C, (f) 110°C and (g) 120°C.

4. Conclusions

The LC alignment properties of *n*-alkylsulphonyl-substituted polyoxyethylenes were found to be affected by *n*-alkyl chain length and rubbing density. When the number of carbon atoms in the *n*-alkyl side group of the #S-PEO films was larger than eight, homeotropic LC alignment behaviour with tilt angles of about 90° on the unrubbed #S-PEO surfaces was observed. The LC cells made from the 8S-PEO and 10S-PEO films on glass and plastic substrates maintained their homeotropic LC aligning ability for at least 6 months

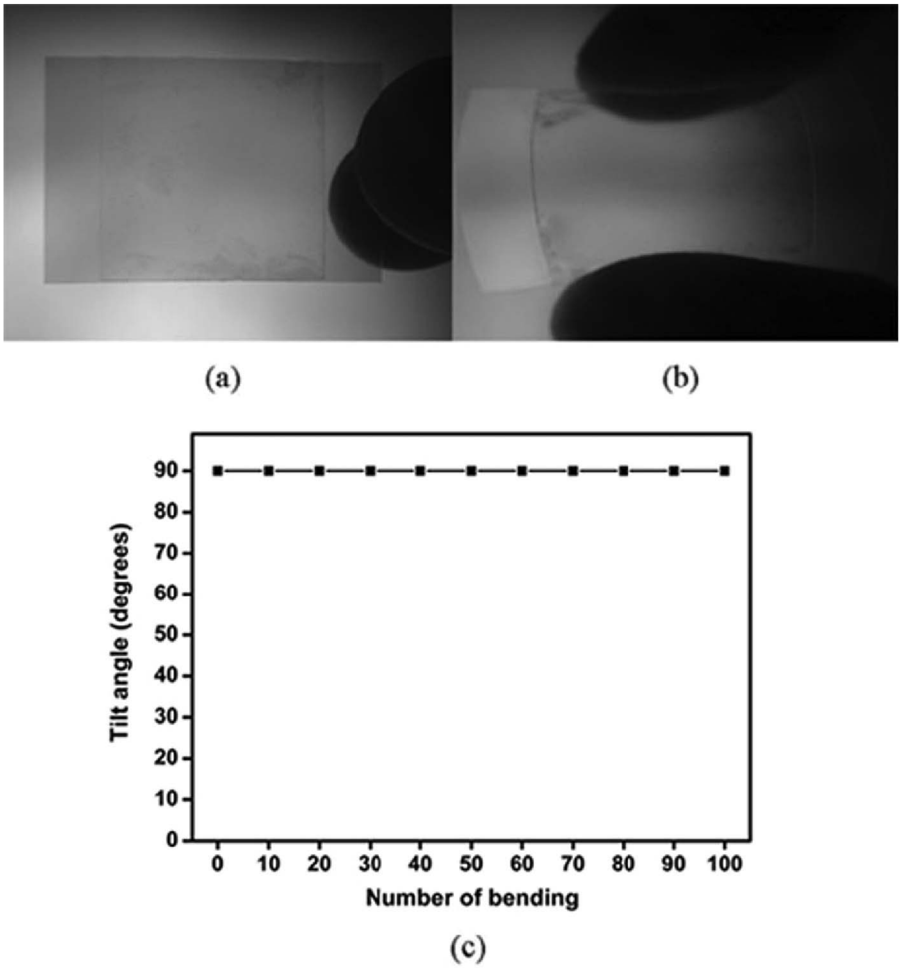

Figure 9. Photo images of the (a) unbent and (b) bent LC cell made from 10S-PEO film on polyethylene terephthalate substrate and (c) tilt angles of the LC cell as a function of number of bending.

(from the time when the LC cells were initially made) and those made from the same polymer films on PET substrates maintained their LC aligning ability after bending them 100 times.

Acknowledgement

Financial support by the Engineering Research Institute at Seoul National University, Korea Research Foundation through the Basic Research Program (Grant No. KRF-2008-314-D00112), and Soongsil University are gratefully acknowledged.

References

(1) Kohki, T.; Masaki, H.; Mitsuhiro, K.; Nobuyuki, I.; Ray, H.; Masanori, S. *Alignment Technologies and Applications of Liquid Crystal Devices*; Taylor & Francis: New York, 2005.
(2) Ichimura, K. *Chem. Rev.* **2000**, *100*, 1847–1874.
(3) O'Neill, M.; Kelly, S.M. *J. Phys. D: Appl. Phys.* **2000**, *33*, R67–R84.
(4) Chaudhari, P.; Lacey, J.; Doyle, J.; Galligan, E.; Lien, S.-C.A.; Callegari, A.; Hougham, G.; Lang, N.D.; Andry, P.S.; John, R.; Yang, K.-H.; Lu, M.; Cai, C.; Speidell, J.; Purushothaman, S.; Ritsko, J.; Samant, M.; Stohr, J.; Nakagawa, Y.; Katoh, Y.; Saitoh, Y.; Sakai, K.; Satoh, H.; Odahara, S.; Nakano, H.; Nakagaki, J.; Shiota, Y. *Nature* **2001**, *411*, 56–59.
(5) Kim, J.-H.; Yoneya, M.; Yokoyama, H. *Nature* **2002**, *420*, 159–162.
(6) Varghese, S.; Narayanankutty, S.; Bastiaansen, C.W.M.; Crawford, G.P.; Broer, D.J. *Adv. Mater.* **2004**, *16*, 1600–1605.
(7) Yaroshchuk, O.; Zakrevskyy, Y.; Kumar, S.; Kelly, J.; Chien, L.-C.; Lindau, J. *Phys. Rev. E*, **2004**, *69*, 011702/1–011702/7.
(8) Gu, M.; Smalyukh, I.I.; Lavrentovich, O.D. *Appl. Phys. Lett.* **2006**, *88*, 061110/1–061110/3.
(9) Yi, Y.; Nakata, M.; Martin, A.R.; Clark, N.A. *Appl. Phys. Lett.* **2007**, *90*, 163510/1–163510/3.
(10) Vaughn, K.E.; Sousa, M.; Kang, D.; Rosenblatt, C. *Appl. Phys. Lett.* **2007**, *90*, 194102/1–194102/3.

(11) Kim, J.B.; Choi, C.J.; Park, J.S.; Jo, S.J.; Hwang, B.H.; Jo, M.K.; Kang, D.; Lee, S.J.; Kim, Y.S.; Baik, H.K. *Adv. Mater.* **2008**, *20*, 3073–3078.

(12) Lee, K.-W.; Paek, S.-H.; Lien, A.; Durning, C.; Fukuro H. *Macromolecules* **1996**, *29*, 8894–8899.

(13) Paek, S.-H.; Durning, C.J.; Lee, K.-W.; Lien, A. *J. Appl. Phys.* **1998**, *83*, 1270–1280.

(14) Paek, S.-H. *J. Ind. Eng. Chem.* **2001**, *7*, 316–325.

(15) Ree, M. *Macromol. Res.* **2006**, *14*, 1–33.

(16) Seo, D.-S.; Kobayashi, S.; Nishikawa, M.; Kim, J.-H.; Yabe, Y. *Appl. Phys. Lett.* **1995**, *66*, 1334–1336.

(17) Lee, S.W.; Kim, S.I.; Park, Y.H.; Ree, M.; Rim, Y.N.; Yoon, H.J.; Kim, Y.B. *Mol. Cryst. Liq. Cryst.* **2000**, *349*, 271–274.

(18) Lee, S.J.; Jung, J.C.; Lee, S.W., Ree, M. *J. Polym. Sci. Part A* **2004**, *42*, 3130–3142.

(19) Lee, S.W.; Lee, S.J.; Hahm, S.G.; Lee, T.J.; Lee, B.; Chae, B.; Kim, S.B.; Jung, J.C.; Zin, W.C.; Sohn, B.H.; Ree, M. *Macromolecueles* **2005**, *38*, 4331–4338.

(20) Lee, S.B.; Shin, G.J.; Chi, J.H.; Zin, W.-C.; Jung, J.C.; Hahm, S.G.; Ree, M.; Chang, T. *Polymer* **2006**, *47*, 6606–6621.

(21) Sarkar, A.; More, A.S.; Wadgaonkar, P.P.; Shin, G.J.; Jung, J.C. *J. Appl. Polym. Sci.* **2007**, *105*, 1793–1801.

(22) Liu, Z.; Yu, F.; Zhang, Q.; Zeng, Y.; Wang, Y. *Eur. Polym. J.* **2008**, *44*, 2718–2727.

(23) Kang, H.; Park, J.S.; Kang, D.; Lee, J.-C. *Polym. Adv. Technol.* **2009**, DOI: 10.1002/pat.1314.

(24) Kang, H.; Kim, T.-H.; Kang, D.; Lee, J.-C. *Macromol. Chem. Phys.* **2009**, *210*, 926–935.

(25) Seo, D.-S. *Liq. Cryst.* **1999**, *26*, 1621–1624.

(26) Malone, S.M.; Schwartz, D.K. *Langmuir* **2008**, *24*, 9790–9794.

(27) Lee, J.-C.; Litt, M.H.; Rogers, C.E. *Macromolecules* **1997**, *30*, 3766–3774.

(28) Lee, J.-C.; Litt, M.H.; Rogers, C.E. *Macromolecules* **1998**, *31*, 2440–2446.

(29) Lee, J.-C.; Litt, M.H.; Rogers, C.E. *J. Polym. Sci. Part A* **1998**, *36*, 793–801.

(30) Cho, K.; Cho, J.H.; Lee, J.-C.; Han, S.-H.; Lee, K.-B.; Koo, J. *Langmuir* **2003**, *19*, 7021–7025.

(31) Cho, K.; Cho, J.H.; Yoon, S.; Park, C.E.; Lee, J.-C.; Han, S.-H.; Lee, K.-B.; Koo, J. *Macromolecules* **2003**, *36*, 2009–2014.

(32) Kim, B.G.; Sohn, E.-H.; Lee, J.-C. *Macromol. Chem. Phys.* **2007**, *208*, 1011–1019.

(33) Chae, B.; Kim, S.B.; Lee, S.W.; Kim, S.I.; Choi, W.; Lee, B.; Ree, M.; Lee, K.H.; Jung, J.C. *Macromolecules* **2002**, *35*, 10119–10130.

(34) Hahm, S.G.; Lee, T.J.; Chang, T.; Jung, J.C.; Zin, W.-C. *Macromolecules* **2006**, *39*, 5385–5392.

(35) Owens, D.K.; Wendt, R.C. *J. Appl. Polym. Sci.* **1969**, *13*, 1741–1747.

(36) Sprokel, G.J. *The Physics and Chemistry of Liquid Crystal Devices*; Springer: New York, 1980.

(37) Turi, E.A. *Thermal Characterization of Polymeric Materials*; Academic Press: London, 1981.

(38) Shi, H.; Zhao, Y.; Zhang, X.; Zhou, Y.; Xu, Y.; Zhou, S.; Wang, D.; Han, C.C.; Xu, D. *Polymer* **2004**, *45*, 6299–6307.

(39) Seo, J.-H.; Hwang, S.W.; Song, D.H.; Shin, J.H.; Yoon, T.-H.; Kim, J.C. *J. Phys. Chem. B* **2009**, *113*, 2001–2005.

(40) Brandrup, J.; Immergut, E.H.; Grulke, E.A. *Polymer Handbook*; J. Wiley: New York, 1999.

(41) Crawford, G.P. *Flexible Flat Panel Displays*; J. Wiley: Chichester, 2005.

(42) Retsos, H.; Lee, D.; Lim, M.-Y.; Lee, J.-C.; Char, K.; Creton, C. *Langmuir* **2008**, *24*, 10169–10173.